Available online at www.sciencedirect.com
SCIENCE DIRECT®
Journal of Chromatography A, 1054 (2004) 293–301
JOURNAL OF CHROMATOGRAPHY A
www.elsevier.com/locate/chroma

Characterization of winemaking yeast by cell number–size distribution analysis through flow field-flow fractionation with multi-wavelength turbidimetric detection

Andrea Zattoni[a], Dora Melucci[a], Pierluigi Reschiglian[a,*], Ramsés Sanz[b], Lluís Puignou[b], Maria Teresa Galceran[b]

[a] *Department of Chemistry "G. Ciamician", University of Bologna, Via Selmi 2, I-40126 Bologna, Italy*
[b] *Department of Analytical Chemistry, University of Barcelona, Martí i Franquès 1-11, E-08028 Barcelona, Spain*

Available online 16 September 2004

Abstract

Yeasts are widely used in several areas of food industry, e.g. baking, beer brewing, and wine production. Interest in new analytical methods for quality control and characterization of yeast cells is thus increasing. The biophysical properties of yeast cells, among which cell size, are related to yeast cell capabilities to produce primary and secondary metabolites during the fermentation process. Biophysical properties of winemaking yeast strains can be screened by field-flow fractionation (FFF). In this work we present the use of flow FFF (FlFFF) with turbidimetric multi-wavelength detection for the number–size distribution analysis of different commercial winemaking yeast varieties. The use of a diode-array detector allows to apply to dispersed samples like yeast cells the recently developed method for number–size (or mass–size) analysis in flow-assisted separation techniques. Results for six commercial winemaking yeast strains are compared with data obtained by a standard method for cell sizing (Coulter counter). The method here proposed gives, at short analysis time, accurate information on the number of cells of a given size, and information on the total number of cells.
© 2004 Elsevier B.V. All rights reserved.

Keywords: Food analysis; Wine; Yeast; *Saccharomyces*; Flow field-flow fractionation; Particle-size distribution analysis; Multi-wavelength turbidimetry

1. Introduction

Yeast is widely used in several areas of food industry. The genus *Saccharomyces* is the most frequently employed in baking, beer brewing, and wine production. In winemaking, the transformation of grape juice into wine is essentially a microbial process driven by yeast [1]. The availability of ready-to-use, commercial strains of *Saccharomyces cerevisiae* and *Saccharomyces bayanus* has prompted their widespread use in wine production. Significant improvements in the quality of wine are related to the "best" selection of yeast strains to be used as fermentation starters [2]. Moreover, several advantages such as fast start, uniform and full fermentation, low levels of residual sugars, and total microbiological control have been observed [3]. For these reasons the development of methods for the identification and characterization of yeast is needed.

Field-flow fractionation (FFF) is a family of flow-assisted, separation techniques able to fractionate and characterize macromolecular and supramolecular species from macromolecules to micron-sized particles, among which cells [4]. In the past few years, different FFF subtechniques have been applied to separate yeast cells [5–7]. New methodologies for the characterization of commercial active, dry winemaking yeast by sedimentation FFF (SdFFF) were developed. They were based either on centrifugal SdFFF [8] or on gravitational FFF (GrFFF), the low-cost subset of FFF that employs Earth's gravity to generate the applied field [9–11]. Such methods were proved able to fingerprint different commercial winemaking yeast strains, and to follow biophysical modifications of the yeast cells that reflect into differences in the fractographic profiles. Since yeast cell biophysical features such as size, shape, and density can be related to via-

* Corresponding author. Tel.: +39 051 2099564; fax: +39 051 2099456.
E-mail address: pierluig.reschiglian@unibo.it (P. Reschiglian).

0021-9673/$ – see front matter © 2004 Elsevier B.V. All rights reserved.
doi:10.1016/j.chroma.2004.07.088

Nomenclature

A	absorbance (–)
b	optical cell path length (cm)
c	sample mass concentration (g cm^{-3})
d	particle diameter (cm)
d_e	elution-equivalent diameter (cm)
d_x	size distribution percentiles (μm)
$f(d)$	mass–size distribution (g cm^{-1})
$f_n(d)$	number–size distribution (particles cm^{-1})
F_c	FlFFF cross-flow rate (cm^3 min^{-1})
F_{in}	FlFFF longitudinal flow rate (cm^3 min^{-1})
K	extinction coefficient (cm^2 g^{-1})
m	mass of eluted particles (g)
m_p	particle relative refractive index (–)
n	refractive index of the dispersing medium (–)
n_0	eluted particle number (–)
n_p	particle refractive index (–)
N	particle number concentration (particles cm^{-3})
Q	extinction efficiency (–)
R_x	correlation coefficients
S_d	diameter-based size selectivity (–)
t_r	retention time (s)
V_0	void volume (cm^3)
V_r	retention volume (cm^3)
V_{r1}	extrapolated retention volume for a particle of unit diameter (cm^3)
x	size parameter (–)
y	input values for system solution
α	particle density (g cm^{-3})
λ	incident wavelength in the dispersing medium (cm)
λ_0	incident wavelength in the vacuum (cm)
τ	turbidity (cm^{-1})

bility [12] and growth cycle of the yeast cells, the obtained fractograms can be eventually related to aspects of winemaking yeast quality and, consequently, to the quality of wines.

Quantitative information is generally important for the applicability of FFF methods to cell characterization. For instance, sample recovery evaluation is a fundamental requisite for the applicability of FFF methods to living cells [13]. The quantitative response, in terms of size and number of the fractionated cells, is thus needed to develop an effective FFF approach for the characterization of commercial yeast varieties. To obtain quantitative response from FFF of yeast samples, a method is first of all required to convert the turbidimetric response obtained from the UV/vis detector to mass, volume or number of the fractionated cells. Different approaches, based on the derivation of the Beer–Lambert law for flow-through turbidimetric measurements, have been developed for the application to FFF analysis of dispersed samples [14–17]. These methods require the evaluation of the analyte optical properties either by experimental calibration with monodispersed standard samples [14], or by prediction through an optical model [15,16]. Because the extinction properties of dispersed samples are size-dependent, calibration-based methods should however require monodispersed standards, the availability of which is often limited. On the other hand, the extinction coefficient of dispersed samples can generally be predicted by applying a model such as the Mie scattering theory or other simpler, approximate approaches that can be applied only within limited domains of sample features [18]. However, any model-based prediction of the optical properties of dispersed analytes requires either the exact knowledge of sample specifications (i.e. size, shape, refractive index, density) or restriction of the range of experimental and instrumental conditions within which the optical properties can be considered relatively constant [15]. For complex samples such as yeast cells the above requisites are hardly met.

The GrFFF approaches up to now developed for winemaking yeast characterization have mostly resulted into qualitative fingerprinting of the yeast strains, because of evident differences of the fractogram profiles due to differences in all the cell biophysical features, among which size. Yeast cell size is an important physical parameter since it can be related to the growth stage of yeast cells and, then, to fermentation performance [12]. Nevertheless, the complex dependence of GrFFF retention on all the biophysical features of sample particles has hindered the direct conversion of cell retention time into yeast cell size. This was confirmed when GrFFF–UV/vis fractograms of winemaking yeast samples have been compared to size data obtained with uncorrelated methods such as Coulter counter [11] and, finally, when centrifugal SdFFF was coupled with flow cytometry [8].

Flow FFF (FlFFF) shows simpler than other FFF techniques for sizing purposes, since FlFFF retention is relatively independent of density. This is because of the non-specific, hydrodynamic field across the channel, which is generated by the application of a secondary mobile phase flow that drives sample components towards the channel accumulation surface [19]. FlFFF can fractionate cells with analysis time shorter than in GrFFF, according to the hydrodynamic radius of the analyte particles and independently of cell density [20]. Using FlFFF then allows to better develop quantitative FFF methods for directly sizing yeast cells.

In this work, we present FlFFF with UV/vis diode-array detection (DAD) to obtain quantitative characterization of different commercial winemaking yeast varieties via the independent evaluation of their particle size–number distribution and optical properties of the yeast cells. UV/vis DAD allows to apply the original method for quantitative analysis in flow-assisted separation of dispersed samples, which we have recently developed and up to now tested just with a few FFF cases [21]. The method experimentally obtains the optical properties of the analyte without requiring standards for calibration or a model that needs knowledge of sample

specifications, and it then allows to independently obtain the mass–size (or number–size) particle distribution (what we named the particle size–amount distribution, PSAD [14]) of the analyte from a single separation experiment. The method is based on the fundamental property of the extinction efficiency to be a function of the ratio between the diameter of dispersed, spherical particles and the incident wavelength, when the particle relative refractive index (i.e. the ratio between particle refractive index and refractive index of the dispersing medium) is constant [18]. The use of UV/vis DAD is thus the first requisite since the method requires to register turbidity as a function of the incident wavelength. Conversion from retention volume to the size of fractionated yeast cells is then obtained through the evaluation of size selectivity via calibration with standards of known size and shape. In our case, the calibration procedure makes use of standard spherical, rigid polystyrene (PS) particles whose shape is different than yeast cell shape. Since retention in FlFFF is dependent on particle shape, the cell size is expressed in terms of "elution-equivalent diameter", which is here defined as the diameter of a standard, spherical particle that is eluted at the same retention volume as the cell. Once the cell retention volumes have been converted into elution-equivalent cell size values by means of the obtained elution-based size selectivity, the method is applied to the multi-wavelength, turbidimetric FlFFF fractograms of yeast samples to obtain PSAD (as number–size distribution) analysis. The final problem in independently obtaining the extinction efficiency and number–size distribution functions for each sample is solved by solving a non-linear equation system, by means of the numerical method we have proposed and tested in a previous paper [21]. Six different yeast strains from different species of Saccharomyces were analyzed, and the size distribution results were compared to sizing data obtained through the electrosensing zone technique (i.e. the Coulter counter, CC), a reference method for particle-size distribution (PSD) analysis of particles, among which cells. Though CC is an indirect method for PSD analysis, and it is not as accurate as an absolute method like microscopy, CC is widely used for routine PSD analysis because of its operation simplicity and short analysis times. In this work, we aim, in fact, to evaluate, rather than the absolute accuracy of the FlFFF/PSAD sizing data, the correlation degree existing between the FlFFF/PSAD results and the results obtained through a widely-employed method for routine PSD analysis.

2. Experimental

2.1. FlFFF

The FlFFF system was similar to the system employed in previous work [22]. The channel was a prototype version derived from the commercial model F-1000 Universal Fractionator (FFFractionation LLC, Salt Lake City, UT). The accumulation wall was made of a sheet of regenerated cellulose membrane with a 1000 M_r cutoff. The channel was held in vertical position to prevent the influence of gravity on the perpendicular field. Nominal channel dimensions were 30.0 cm in tip-to-tip length and 2.0 cm in breadth, with a 0.0207-cm thickness. Nominal channel volume was 1.41 cm^3. Sample injection was made at an injection flow rate of 2.0 $cm^3\,min^{-1}$ through a Rheodyne valve, model 7125 (Rheodyne, Cotati, CA), with a calibrated loop volume of 17.83 ± 0.06 μL (N = 30). The longitudinal flow rate (F_{in}) was always 4.0 $cm^3\,min^{-1}$, and it was generated by an SSI Series II pump (SSI, State College, PA). The required external field was generated by a mobile phase cross-flow rate (F_c) of 1.0 $cm^3\,min^{-1}$, which was delivered by a Varian pump, model 2510 (Varian, Walnut Creek, CA). Two 4-way valves were employed: the first valve to switch between the two cross-flow modes (recirculating, non recirculating), the second valve to switch between the two longitudinal flow modes (direct and back-flushing). One 6-way Valco valve model E60-230 (VICI, Onsala, Sweden) was employed to switch between stop-flow mode and run mode. The stop-flow time was 85 s. For channel cleaning, a back-flushing step at 10.0 $cm^3\,min^{-1}$ with the cross flow switched off was applied after each elution. Mobile phase was pure Milli-Q grade water produced by Simplicity 185 (Millipore, Bedford, MA) added with 0.02% (w/v) sodium azide (NaN_3, Sigma–Aldrich, Steinheim, Germany), 0.1% (w/v) Triton X-100 (Fluka, Buchs, Switzerland) and 3 mM phosphate-buffered saline (PBS) at pH 7.4. The UV/vis detector was the model UV6000LP DAD spectrophotometer (Thermo Finnigan, Austin, TX) operating at a wavelength range of 250–700 nm. The cell path length was measured with a spectroscopic standard, as described in a previous work [23]. The result was 4.6 ± 0.3 cm. Detection parameters and signal acquisition were controlled by the ChromQuest Chromatography Software (version 2.51, Thermo Finnigan).

2.2. Samples

Size calibration in FlFFF was performed with NIST/traceable, polystyrene (PS) standard microspheres (Duke Scientific, Palo Alto, CA) of 2.013 ± 0.025 μm, 3.063 ± 0.027 μm, 4.000 ± 0.033 μm, 6.992 ± 0.050 μm, and 9.975 ± 0.061 μm diameter. Coulter counter instrumental calibration was performed with 18.5-μm Calibration Standard PS Latex (Coulter Electronics Ltd., Luton, Beds, England). Yeast samples were six different types of active dry winemaking yeast from different species of *Saccharomyces*. From *Saccharomyces cerevisiae*: Intec Red and Intec Cerevisiae. From *Saccharomyces uvarum*: Uvaferm UVA. From *Saccharomyces bayanus*: Intec Bayanus, Vitilevure and Uvaferm PM. They were supplied by Tensum Ibérica, S.L. (Martorell, Barcelona, Spain). For FlFFF, the samples were dispersed using sonication (2 min) at 0.1% (w/v) in isotonic NaCl, centrifuged at 1000 rpm for 3 min to discard possible culture broth residues, and then centrifuged again at 6000 rpm for 6 min to precipitate the yeast cells. After this process, yeast cells were cleaned twice with the isotonic

NaCl and re-suspended in 1 mL of the carrier liquid, they were kept at 4 °C before analysis, and sonicated for 30 s before injection into the FlFFF system. All injections were made at room temperature.

2.3. CC analysis

CC size measurements were performed using a Multisizer II (Coulter Corporation, Hialeah, FL) set for 256-channel analysis. Aperture size was 70 μm (measure rank: from 2 to 60% of the nominal aperture size) and the aperture current was 1600 μA. Yeast samples were dispersed in PBS before the measurements, and then diluted with the conducting fluid Isoton II solution (Coulter Corporation). Intec Bayanus, Intec Cerevisiae and Vitilevure yeast samples were dispersed at a concentration of 0.05% (w/v), and diluted 1:1000 in Isoton II. Intec Red (dispersed at 0.2%, w/v), Uvaferm PM and Uvaferm UVA (both dispersed at 0.3%, w/v) were diluted 1:10,000 in Isoton II. The analytical volume was 500 μL, and the average of three replicates was considered ($N = 3$).

3. Methods

3.1. Conversion from retention to size

The first step required for the application of the PSAD method is the conversion from retention volume to cell size. Cells are eluted in FFF according to the steric/hyperlayer (st/hyp) mechanism [24], for which a theoretical relationship between retention and size of the sample particles is not available. The conversion can be thus performed by experimental determination of the diameter-based size selectivity, S_d (–), which is defined as:

$$S_d = \left| \frac{\partial \log V_r}{\partial \log d} \right| \tag{1}$$

where V_r (cm^3) is the particle retention volume and d (cm) the particle diameter [25]. It has been experimentally found that, in st/hyp FFF, $\log V_r$ linearly depends on $\log d$ [22,26–28]. Within the size range in which it is independent of d, S_d can be determined as the absolute value of the slope of a linear regression plot of $\log V_r$ versus $\log d$:

$$\log V_r = -S_d \log d + \log V_{r1} \tag{2}$$

where V_{r1} (cm^3) is the extrapolated retention volume for a particle of unit diameter. Eq. (2) can be rearranged as:

$$d_i = \left(\frac{V_{r,i}}{V_{r1}} \right)^{-1/S_d} \tag{3}$$

where $V_{r,i}$ (cm^3) is the retention volume of the i-th digitized point in the fractogram. Eq. (3) gives conversion of retention volume values into particle diameter values (d_i). Since in FlFFF retention is independent of sample density, size selectivity can be determined with standard particles of density different from sample particle density.

In fact, particles such as yeast cells can be different from the standard particles not only in density but also in other biophysical features (e.g. shape, rigidity, budding) and, then, in terms of the hydrodynamic behavior. As a consequence, Eq. (3) can be used for FlFFF sizing if a definition of elution-equivalent diameter (d_e) is introduced. The elution-equivalent diameter can be defined as the diameter of a rigid, spherical particle which is eluted at the same retention volume as the sample particle. Eq. (3) can be then re-written as:

$$d_{e,i} = \left(\frac{V_{r,i}}{V_{r1}} \right)^{-1/S_d} \tag{4}$$

which can be used in FlFFF sizing of yeast cells with size calibration performed with standard, spherical particles such as PS beads. Once S_d is determined with PS beads of known size, cell size in terms of d_e can be then obtained from FlFFF retention.

3.2. Multi-wavelength PSAD analysis

The method for PSAD analysis with multi-wavelength turbidimetric detection has been fully presented in a recent paper [21]. Since the first application to a real sample such as yeast cells is here for the first time presented, we describe here below the method fundamentals for this specific application.

The turbidity of a dispersed sample τ (cm^{-1}) can be experimentally obtained from the instrumental signal of a UV/vis detector that operates as a turbidimeter [17]:

$$\tau = \frac{1}{b} \ln(10) A \tag{5}$$

where b (cm) is the optical cell path length, and A (–) the instrumental absorbance signal. We can express τ as:

$$\tau = \ln(10) K c \tag{6}$$

where c ($g\,cm^{-3}$) is the sample mass concentration, and K ($cm^2\,g^{-1}$) the sample extinction coefficient, which we proved to be independent of c in a broad range of dilute dispersions [29].

In a dispersion of spherical particles, τ is a function of particle diameter d, number concentration of the particles N (particles cm^{-3}) and of the dimensionless quantity Q (–), the extinction efficiency [18].

$$\tau = \frac{\pi}{4} d^2 N Q \tag{7}$$

A fundamental property of Q states that, at constant particle shape, Q is a function of the type $Q(x, m_p)$, where x is the size parameter defined as $x = \pi d/\lambda$, in which λ (cm) is the incident wavelength in the dispersing medium, which is $\lambda = \lambda_0/n$ where λ_0 (cm) is the wavelength in the vacuum and n (–) the refractive index of the dispersing medium [18]. The parameter m_p (–) is the particle relative refractive index, defined as $m_p = n_p/n$, where n_p (–) is the particle refractive index. At constant m_p, $Q = Q(x)$. Then, by combining Eqs. 6

and 7 one gets

$$K = \frac{3Q(x)}{2\ln(10)\alpha d} \tag{8}$$

where α (g cm^{-3}) is the particle density.

When in flow-assisted, size separation of dispersed samples the retention time axis can be converted into sample size values via a model or an empirical relationship, the PSD of the sample can be obtained by transformation of the analytical signal recorded as a function of time, as shown in previous work [30]. In the case of FlFFF with turbidimetric detection, the expression of τ in Eq. (6) can be rewritten as a function of the retention volume V_r and of the mass m (g) of the eluted particles:

$$\tau = \ln(10) K \frac{\partial m}{\partial V_r(d)} \tag{9}$$

From the definition of mass–size distribution $f(d)$ (g cm^{-1}) one gets:

$$f(d) \stackrel{def}{=} \frac{\partial m}{\partial d} = \frac{\partial m}{\partial V_r(d)} \frac{\partial V_r(d)}{\partial d} \tag{10}$$

By combining Eqs. (9) and (10), and substituting the expression for K in Eq. (8), we obtain:

$$f(d) = \frac{2}{3} \frac{\tau \alpha d}{Q(x)} \frac{\partial V_r(d)}{\partial d} \tag{11}$$

The correspondent expression for the number–size distribution $f_n(d)$ (particles cm^{-1}) can be easily obtained by dividing Eq. (11) by the particle mass $(\pi/6)d^3\alpha$. It results in the following:

$$f_n(d) = \frac{4\tau d}{\pi d^2 Q(x)} \frac{\partial V_r(d)}{\partial d} \tag{12}$$

When turbidimetric detection is performed through a UV/vis DAD, τ can be recorded as a function of both V_r and λ. If we assume that V_r values can be converted into particle size values as described in the previous section, we have $\tau = \tau(d, \lambda)$. Hence,

$$f_n(d)Q(x) = f_n(d)Q\left(\frac{\pi d}{\lambda}\right) = y(d, \lambda) \tag{13}$$

$$y(d, \lambda) = \frac{4\tau}{\pi d^2} \frac{\partial V_r}{\partial d} \tag{14}$$

In Eq. (13), the $y(d, \lambda)$ values are the experimental values from which the values for $f_n(d)$ and $Q(x)$ can be computed. Eq. (14) shows that the $y(d, \lambda)$ values can be obtained by experimentally measuring the turbidity values τ (V_r, λ). Conversion from retention to size then gives τ ($d(V_r)$, λ) and $\partial V_r(d)/\partial(d)$. Details on the numerical procedure to handle the experimental values of τ (V_r, λ), and to solve the system in Eq. (13), are given in Ref. [21], and summarized in the next section.

Some conditions must be given for the application of Eqs. (13) and (14) to real samples. First, they are valid for particles of constant relative refractive index (m_p), that is for particles which neither absorb light at a specific wavelength nor show different absorbance values at different incident wavelengths. Second, to apply Eqs. (13) and (14) to non-standard particles, it must be assumed that the d_e values for the eluted particles correspond to their optical diameter values, which are used in Eqs. (13) and (14). In fact, the optical diameter is the diameter of a circle with the same surface area as the average cross-section of the particle.

It must be finally pointed out that, since $f_n(d)$ is not a normalized frequency function, the obtained number–size distribution actually is also a function of the total number of the eluted particles n_0 (–), since:

$$\int_0^\infty f_n(d)\mathrm{d}d = n_0 \tag{15}$$

Application of the method thus requires that, in order to compute $f_n(d)$, the eluted particle number (n_0) after the separation–detection process is determined by an independent measurement.

3.3. Data handling

Raw data of multi-wavelength fractograms were exported as a text file through the proprietary detector software. The text file is a matrix of spectrophotometric signal (absorbance, A_{ij}), retention time ($t_{r,i}$, (s)) and wavelength ($\lambda_{0,j}$) values. Experimental data were converted into a suitable form, and used as input data for the numerical solution of the system in Eq. (13) through the following steps of a home-written Matlab routine (Matlab 6.0, The Mathworks, Natick, MA):

- $\lambda_{0,j}$ values are divided by the mobile phase refractive index n to convert $\lambda_{0,j}$ values in air into λ_j values in the dispersing medium;
- $t_{r,i}$ values are converted to retention volume values $V_{r,i}$, via the elution flow rate (F_{in}) value;
- correction for baseline drift is performed, and the void peak is removed by extrapolating the profile from the saddle point between the void peak and the first sample peak to zero at $V_{r,i} = V_0$;
- fractogram noise due to pump instability is removed from the absorbance signal by filtering the frequency trasform of the V_r domain. In fact, we have proved that the numerical method is able to reduce noise intensity, either in case of white noise or noise proportional to the signal intensity [21]. Nonetheless, structured noise in the V_r (or diameter) domain is not affected by the numerical treatment, and it must be removed before the system solution;
- $V_{r,i}$ values are converted to elution-equivalent diameter values $d_{e,i}$ via Eq. (3);
- A_{ij} values are divided by $\ln(10)b$, where b is the cell pathlength, to obtain the turbidity values τ_{ij} (see Eqs. (5) and (6);
- τ_{ij} values are converted to y_{ij} values (i.e. the product of f_n and Q), via Eq. (12);

– d_i, λ_j vectors and y_{ij} matrix are used as input data of the system given by Eq. (13) in the discretized form:

$$f(d_i)Q\left(\frac{\pi d_i}{\lambda_j}\right) = y(d_i, \lambda_j) \quad (16)$$

– solution of the system in Eq. (16) is performed through the numerical routine we developed, optimized and tested in previous work [21].

4. Results and discussion

4.1. FlFFF–DAD/PSAD of yeast strains

Conversion of retention volume (V_r) to elution-equivalent diameter (d_e) values was performed through S_d evaluation (Eq. (3)). Calibration was performed with a mixture of PS standard particles in the diameter range 2–10 μm to cover the diameter range of yeast cells. Under the chosen flow conditions (F_{in} = 4.0 cm^3 min^{-1}, F_c = 1.0 cm^3 min^{-1}, recirculating mode [22]), as predicted for the st/hyp elution mode the PS particles were eluted in reversed order with respect to size, with the largest particles eluted first [24]. Linear regression analysis of V_r values at the peak maxima versus particle diameter (d) values (see Eq. (2)) gave: log V_r (cm^3 min^{-1}) = −(1.07 ± 0.05)log d (μm) + (1.65 ± 0.04) (R^2 = 0.996, P = 95%, N = 10). The S_d value thus results to be 1.07 ± 0.05. This value agrees with the S_d values already found by us in previous FlFFF work on PS micron-sized particles, which made use of the same FlFFF channel [22].

Yeast samples were fractionated under the same flow conditions used for the PS standards, and multi-wavelength fractograms were recorded in the λ range 250–700 nm. Fig. 1 shows the fractograms obtained for the six strains at a selected wavelength (330 nm). Baseline resolution between void peak and yeast cell band was obtained in all cases, and the elution time of the yeast cells was always lower than 6 min. Such analysis time values are slightly shorter than those obtained in previous work on centrifugal SdFFF of yeast [8], and about ten times shorter than those of GrFFF [9–11]. This confirms the ability of FlFFF to achieve fractionation of micronsized particles at the shortest fractionation times [22,28].

Multi-wavelength fractograms were numerically processed as described in Section 3.3. The required value of n_0 (see Eq. (15)) was obtained by evaluation of sample recovery. Sample recovery was determined by off-channel injection of the same sample amount injected to obtain the fractogram, as the ratio between in-channel and off-channel peak areas. Results of the numerical solution were the sample extinction efficiency (Q) and the number–size distribution (f_n) functions, which are respectively shown in Figs. 2 and 3. The Q profiles result not to be significantly different from strain to strain, with Q values around unity at x = 40. This is not surprising, since Q basically depends, at a given x value, on particle shape and on the value of the relative refractive index of cells, which

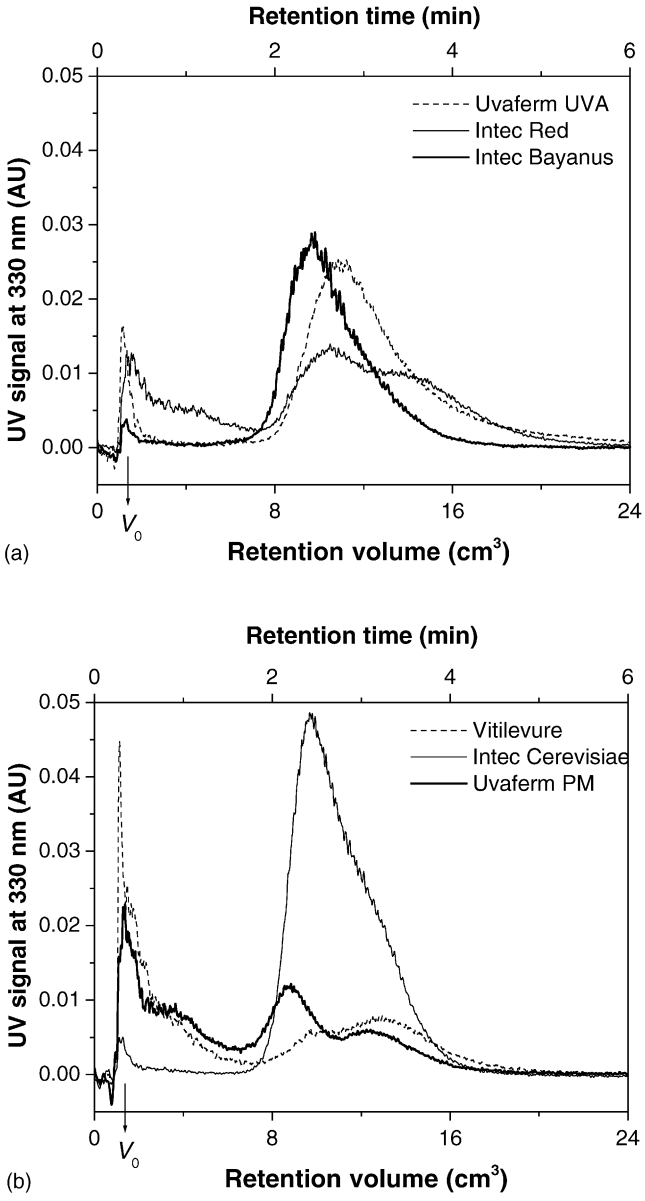

Fig. 1. FlFFF fractograms for different winemaking yeast samples. Experimental conditions are given in Section 2. (a) Uvaferm UVA (dashed line); Intec Red (thin line); Intec Bayanus (thick line); (b) Vitilevure (dashed line); Intec Cerevisiae (thin line); Uvaferm PM (thick line).

should not be significantly different from strain to strain. Values for Q close to unity were also found for other type of cells (human red blood cells [21]), in agreement with the scattering theory of non-absorbing particles [18]. The solutions for f_n (Fig. 3) gave what we call the PSAD profiles.

4.2. FlFFF–DAD/PSAD versus CC/PSD analysis

The information content from the PSAD profiles was evaluated by comparing the results obtained through a reference sizing technique like CC. The same samples whose PSAD profiles are reported in Fig. 3 were then analyzed through CC to get CC/PSD analysis. The results are reported in Fig. 4.

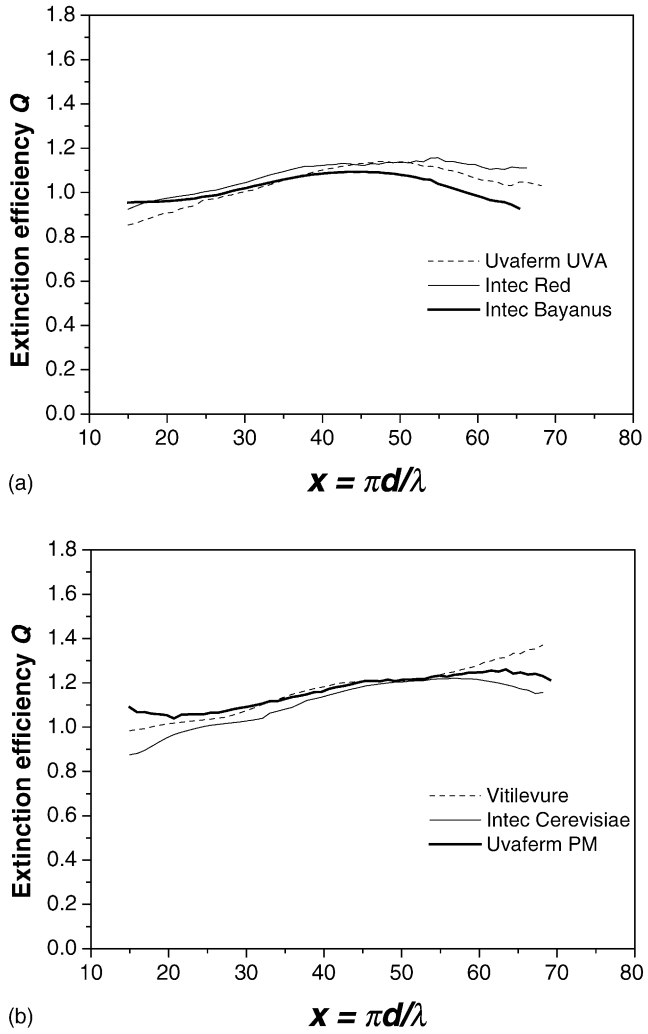

Fig. 2. FlFFF–DAD/PSAD of different yeast types. Output Q functions: (a) Uvaferm UVA (dashed line); Intec Red (thin line); Intec Bayanus (thick line); (b) Vitilevure (dashed line); Intec Cerevisiae (thin line); Uvaferm PM (thick line).

It is worth to mention that CC measures the particle volume, and thus gives cell size in terms of volume-equivalent diameter, that is the diameter of a sphere of same volume as the cell. Nonetheless, FlFFF retention of yeast cells depends on the cell hydrodynamic behavior, which itself depends not only on cell size but also on the other, different biophysical features of the cells, such as cell shape, rigidity and surface characteristics. As a consequence, being S_d determined with spherical PS particles, the obtained PSAD profiles are functions of the elution-equivalent diameter (d_e). High correlation degree between FlFFF–DAD/PSAD and CC/PSD analysis data, that is between volume-equivalent and elution-equivalent diameter values, could prove that, in the case of yeast cells, d_e is not significantly affected by the cell shape, while it mostly depends on the cell volume. To compare CC/PSD and FlFFF–DAD/PSAD analysis, size distribution percentiles (d_{10}, d_{25}, d_{50}, d_{75}, d_{90}) were calculated and compared. Table 1 lists the obtained percentile values, and the

Table 1
Size distribution percentiles of yeast samples: comparison between CC/PSD and FlFFF–DAD/PSAD

Yeast type	CC/PSD (±S.D., N = 3) (μm)					FlFFF–DAD/PSAD (±S.D., N = 3) (μm)					Relative deviation (%)				
	d_{10}	d_{25}	d_{50}	d_{75}	d_{90}	d_{10}	d_{25}	d_{50}	d_{75}	d_{90}	d_{10}	d_{25}	d_{50}	d_{75}	d_{90}
Uvaferm UVA	4.50 (±0.02[a])	4.02 (±0.02[a])	3.54 (±0.02[a])	3.04 (±0.01[a])	2.59 (±0.01[a])	4.24 (±0.05)	3.93 (±0.06)	3.57 (±0.06)	3.16 (±0.05)	2.70 (±0.04)	−5.8	−2.2	0.8	4.1	4.2
Intec Red	4.42 (±0.01)	3.76 (±0.01)	3.14 (±0.003)	2.65 (±0.002)	2.32 (±0.01)	4.38 (±0.02[a])	3.96 (±0.01[a])	3.39 (±0.02[a])	2.84 (±0.03[a])	2.47 (±0.03[a])	−0.9	5.3	7.9	7.4	6.5
Intec Bayanus	5.00 (±0.05)	4.25 (±0.04)	3.60 (±0.03)	2.98 (±0.03)	2.32 (±0.05)	4.70 (±0.09)	4.38 (±0.04)	4.03 (±0.02)	3.61 (±0.02)	3.22 (±0.05)	−5.9	3.0	11.9	21.2	38.9
Vitilevure	5.30 (±0.04)	4.37 (±0.01)	3.55 (±0.03)	2.73 (±0.02)	2.23 (±0.06)	4.08 (±0.15)	3.65 (±0.08)	3.19 (±0.06)	2.81 (±0.05)	2.49 (±0.04)	−23.1	−16.5	−10.2	3.0	11.5
Intec Cerevisiae	4.96 (±0.03)	4.31 (±0.02)	3.70 (±0.02)	3.17 (±0.01)	2.61 (±0.02)	4.47 (±0.12)	4.21 (±0.08)	3.86 (±0.07)	3.42 (±0.06)	3.09 (±0.06)	−9.9	−2.3	4.3	7.9	18.3
Uvaferm PM	5.32 (±0.13[a])	4.81 (±0.10[a])	4.05 (±0.10[a])	3.49 (±0.07[a])	3.05 (±0.05[a])	4.95 (±0.02)	4.60 (±0.03)	4.03 (±0.08)	3.35 (±0.09)	2.85 (±0.07)	−7.0	−4.3	−0.4	−4.1	−6.6

[a] N = 2.

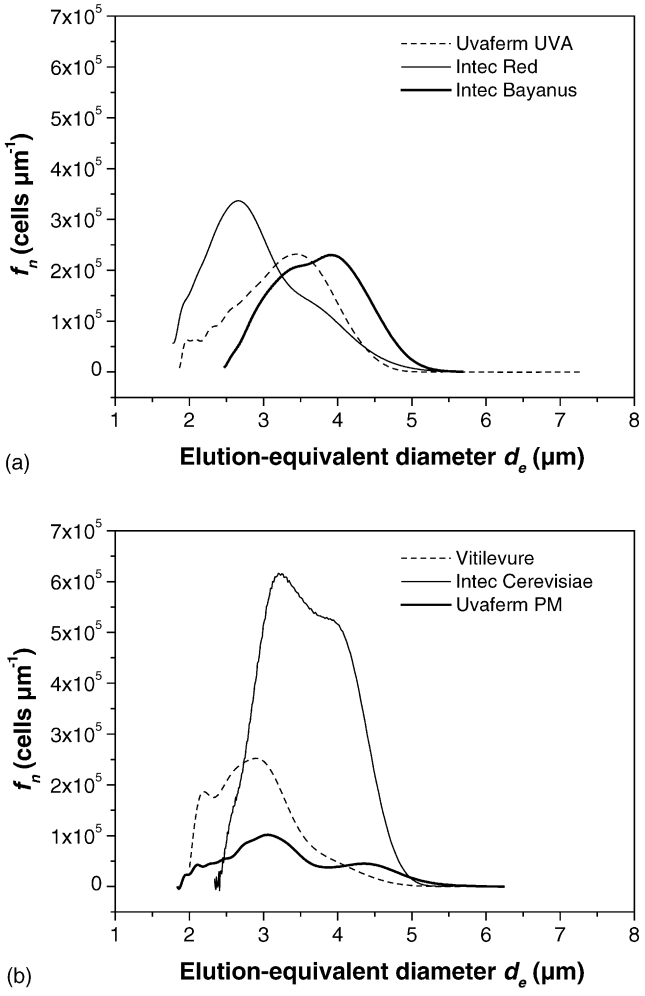

Fig. 3. FlFFF–DAD/PSAD of different yeast types. Output f_n functions: (a) Uvaferm UVA (dashed line); Intec Red (thin line); Intec Bayanus (thick line); (b) Vitilevure (dashed line); Intec Cerevisiae (thin line); Uvaferm PM (thick line).

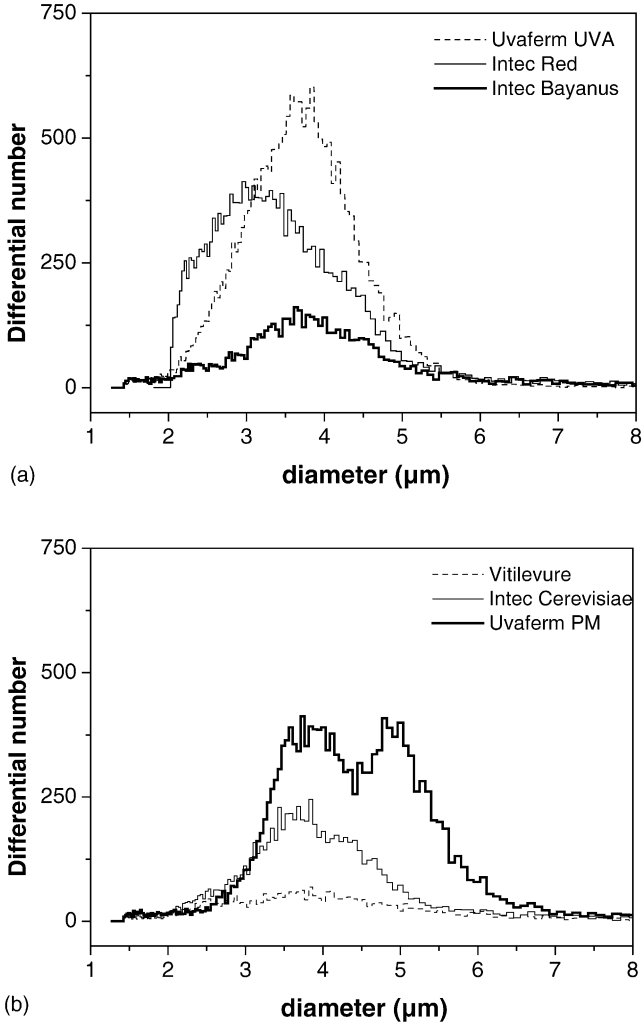

Fig. 4. CC/PSD analysis of different winemaking yeast samples. Experimental conditions are given in Section 2. (a) Uvaferm UVA (dashed line); Intec Red (thin line); Intec Bayanus (thick line); (b) Vitilevure (dashed line); Intec Cerevisiae (thin line); Uvaferm PM (thick line).

percent relative deviations between the corresponding percentile values obtained by the two methods. The run-to-run standard deviation for three repeated runs are also reported for each method. The percent relative standard deviation values (%R.S.D.) calculated for the two methods are comparable, with values ranging from 0.25 to 3% for FlFFF–DAD/PSAD, and from 0.1 to 2.5% for CC/PSD. The %R.S.D. values for FlFFF–DAD/PSAD were also comparable to the %R.S.D. values found in previous work on GrFFF of *S. cerevisiae* for run-to-run variation of the peak area and retention ratio values [11]. In most cases of Table 1, the percent relative deviations between the methods for d_{25}, d_{50} and d_{75} are lower than 10%. It must be recalled that differences as low as 10% in size are quite often obtained by independent methods for PSD analysis [31]. For the Vitilevure and Intec Bayanus strains, the higher percent relative deviation values could be explained by observing the void peaks of the relevant fractograms in Fig. 1. The two fractograms, in fact, present high void peaks, and relatively intense bands at low elution volume (V_r from 2 to 6 cm^3). These intense signals could be due to unretained and poorly retained sample components of, respectively, smaller size than whole cell size like cell debris, proteins or cell metabolites residues, or bigger size like possible cell aggregates [9]. It is noteworthy that such components possibly present in the yeast samples might be separated by FlFFF from whole, single cells, as not to affect PSAD analysis. Since CC is not a separation technique, the presence of non-cellular components or cell aggregates in the sample may in fact affect CC/PSD analysis. As far as the d_{10} and d_{90} values are concerned, higher percent relative deviation values were found in some cases. This finding could confirm that CC/PSD analysis may be affected by the presence of non-cellular sample components or by cell aggregates. Otherwise, the d_{10} and d_{90} values obtained by FlFFF–DAD/PSAD could be less accurate than the other percentile values, since they are more affected by the accuracy of the baseline correction in the multi-wavelength fractograms. This is due to the effect of noise level at the front and the end of the fractogram on the accuracy with which the number of the largest and

smallest cells is determined, being these cells respectively eluted at the front and at the tail of the fractogram. It must be also noted that FlFFF–DAD/PSAD profiles were not corrected for band broadening. Band broadening contribution in the fractograms directly reflects into apparent contribution to the resulting PSAD profiles. As a consequence, even though from percentile analysis the FlFFF–DAD/PSAD profiles do not appear significantly broader than the CC/PSD profiles, possible band broadening effects able to affect to some extent the accuracy of d_{10} and d_{90} values from FlFFF–DAD/PSAD analysis cannot be a priori excluded.

Good correlation between FlFFF–DAD/PSAD and CC/PSD results can finally estimate the ability of the two methods to comparably detect size differences in the yeast cell populations. The correlation coefficients were calculated between percentile values at each percent level (d_x) for the six yeast strains. The results were $R_{10} = 0.665$, $R_{25} = 0.740$, $R_{50} = 0.731$, $R_{75} = 0.670$ and $R_{90} = 0.330$, where R_x is the correlation coefficient for the d_x data set. A *t*-test on R_x values proved that, in all cases except R_{90}, correlation is significant at the 95% confidence level.

5. Conclusions

A new approach based on FlFFF with multi-wavelength detection is applied to number–size distribution analysis of winemaking yeast cells. The FlFFF–DAD/PSAD method determines how many yeast cells of a given size are present in commercial samples of active, dry winemaking yeast. The results are compared to the results obtained through a routine technique for number–size distribution analysis of cells, the CC. Correlation analysis between the two methods indicates that FlFFF–DAD/PSAD analysis generally gives accurate results. With respect to CC/PSD, however, the FlFFF–DAD/PSAD method shows the advantage to be based on a separation technique, the FlFFF, which is able to separate different sample components from whole yeast cells. The results obtained from number–size distribution analysis of yeast cells by FlFFF–DAD can thus be more representative than by CC, and then better related to the quality of winemaking yeast samples. In the future, FlFFF–DAD/PSAD analysis could be effectively used for rapid monitoring of yeast samples to quality assessment purposes. This is because it can determine not only how many cells of a given size but also how many cells are totally present within the gross amount of commercial winemaking yeast samples.

Acknowledgments

Work supported by the International Integrated Actions project number HI-2001-0021 from the Spanish and the Italian governments, by the Italian Ministry of the Education, University and Research (MIUR, COFIN 2002 (MM2002038818_002)), and by the Comissionat per Universitats i Recerca de la Generalitat de Catalunya (CIRIT project number SGR 2001-00057).

References

[1] R.B. Boulton, V.L. Singleton, L.F. Bisson, R.E. Kunkee (Eds.), Principles and Practices of Winemaking, Aspen Publishers, Gaitherburg, MD, 1998, p. 102.
[2] G. Reed, T.W. Nagodawithana, Am. J. Enol. Vitic. 39 (1988) 83.
[3] E. Longo, J.B. Velásquez, C. Sieiro, J. Cansado, P. Calo, T.G. Villa, J. Microbiol. Biotechnol. 8 (1992) 539.
[4] M.E. Schimpf, K. Caldwell, J.C. Giddings (Eds.), Field-Flow Fractionation Handbook, Wiley-Interscience, New York, NY, 2000.
[5] S. Hofstetter-Kuhn, T. Rösler, M. Ehrat, H.M. Widmer, Anal. Biochem. 206 (1992) 300.
[6] M.N. Pons, A. Litzén, G.M. Kresbach, M. Ehrat, H. Vivier, Sep. Sci. Technol. 32 (1997) 1477.
[7] G.H. Markx, J. Rousselet, R. Pethig, J. Liq. Chromatogr. Relat. Technol. 20 (1997) 2857.
[8] R. Sanz, Ph.J.P. Cardot, S. Battu, M.T. Galceran, Anal. Chem. 74 (2002) 4496.
[9] R. Sanz, L. Puignou, P. Reschiglian, M.T. Galceran, J. Chromatogr. A 919 (2001) 339.
[10] R. Sanz, L. Puignou, P. Reschiglian, M.T. Galceran, Am. Biotechnol. Lab. 20 (2002) 46.
[11] R. Sanz, B. Torsello, P. Reschiglian, L. Puignou, M.T. Galceran, J. Chromatogr. A 966 (2002) 135.
[12] R. Sanz, M.T. Galceran, L. Puignou, Biotechnol. Prog. 19 (2003) 1786.
[13] A. Lucas, F. Lepage, P. Cardot, in: M.E. Schimpf, K. Caldwell, J.C. Giddings (Eds.), Field-Flow Fractionation Handbook, Wiley-Interscience, New York, NY, 2000 (Chapter 29).
[14] P. Reschiglian, D. Melucci, A. Zattoni, G. Torsi, J. Microcolumn Sep. 9 (1997) 545.
[15] A. Zattoni, G. Torsi, P. Reschiglian, D. Melucci, J. Chromatogr. Sci. 38 (2000) 122.
[16] P. Reschiglian, D. Melucci, G. Torsi, A. Zattoni, Chromatographia 51 (2000) 87.
[17] P. Reschiglian, A. Zattoni, D. Melucci, G. Torsi, Rev. Anal. Chem. 20 (2001) 239.
[18] H.C. van de Hulst, Light Scattering by Small Particles, Dover Publications, New York, NY, 1981.
[19] S.K. Ratanathanawongs Williams, in: M.E. Schimpf, K. Caldwell, J.C. Giddings (Eds.), Field-Flow Fractionation Handbook, Wiley-Interscience, New York, NY, 2000 (Chapter 17).
[20] P. Reschiglian, A. Zattoni, B. Roda, S. Casolari, M.H. Moon, J. Lee, J. Jung, K. Rodmalm, G. Cenacchi, Anal. Chem. 74 (2002) 4895.
[21] A. Zattoni, E. Loli Piccolomini, G. Torsi, P. Reschiglian, Anal. Chem. 75 (2003) 6469.
[22] P. Reschiglian, D. Melucci, A. Zattoni, L. Malló, M. Hansen, A. Kummerow, M. Miller, Anal. Chem. 72 (2000) 5945.
[23] P. Reschiglian, B. Roda, A. Zattoni, B.-R. Min, M.H. Moon, J. Sep. Sci. 25 (2002) 490.
[24] K. Caldwell, in: M.E. Schimpf, K. Caldwell, J.C. Giddings (Eds.), Field-Flow Fractionation Handbook, Wiley-Interscience, New York, NY, 2000 (Chapter 5).
[25] M.N. Myers, J.C. Giddings, Anal. Chem. 54 (1982) 2284.
[26] S.K. Ratanathanawongs, J.C. Giddings, Anal. Chem. 64 (1992) 6.
[27] J.C. Giddings, M.H. Moon, Anal. Chem. 63 (1991) 2869.
[28] K.G. Wahlund, A. Zattoni, Anal. Chem. 74 (2002) 5621.
[29] P. Reschiglian, D. Melucci, G. Torsi, Chromatographia 44 (1997) 172.
[30] M. Blanda, P. Reschiglian, F. Dondi, R. Beckett, Polym. Int. 33 (1994) 61.
[31] H.G. Barth (Ed.), Modern Methods of Particle Size Analysis, Wiley-Interscience, New York, NY, 1984.